LETTER

doi:10.1038/nature09491

Chronic high-fat diet in fathers programs β-cell dysfunction in female rat offspring

Sheau-Fang Ng[1], Ruby C. Y. Lin[2], D. Ross Laybutt[3], Romain Barres[4], Julie A. Owens[5] & Margaret J. Morris[1]

The global prevalence of obesity is increasing across most ages in both sexes. This is contributing to the early emergence of type 2 diabetes and its related epidemic[1,2]. Having either parent obese is an independent risk factor for childhood obesity[3]. Although the detrimental impacts of diet-induced maternal obesity on adiposity and metabolism in offspring are well established[4], the extent of any contribution of obese fathers is unclear, particularly the role of non-genetic factors in the causal pathway. Here we show that paternal high-fat-diet (HFD) exposure programs β-cell 'dysfunction' in rat F_1 female offspring. Chronic HFD consumption in Sprague–Dawley fathers induced increased body weight, adiposity, impaired glucose tolerance and insulin sensitivity. Relative to controls, their female offspring had an early onset of impaired insulin secretion and glucose tolerance that worsened with time, and normal adiposity. Paternal HFD altered the expression of 642 pancreatic islet genes in adult female offspring ($P < 0.01$); genes belonged to 13 functional clusters, including cation and ATP binding, cytoskeleton and intracellular transport. Broader pathway analysis of 2,492 genes differentially expressed ($P < 0.05$) demonstrated involvement of calcium-, MAPK- and Wnt-signalling pathways, apoptosis and the cell cycle. Hypomethylation of the *Il13ra2* gene, which showed the highest fold difference in expression (1.76-fold increase), was demonstrated. This is the first report in mammals of non-genetic, intergenerational transmission of metabolic sequelae of a HFD from father to offspring.

Increasing evidence indicates an important biological role of fathers in obesity and metabolic programming of their offspring[5,6]. Most human obesity seems to be related to complex gene–environment interactions[7]. Although some alleles associated with obesity are inherited solely from the father[8,9], parental environmental exposures can also affect offspring phenotype[10], with the potential to contribute to the rapid increase in obesity. Susceptibility of the metabolic phenotype to environmentally initiated change also extends into early life through developmental plasticity[10]. In humans, it is difficult to separate the effects of paternal genetic makeup from those of the father's environmental exposures on offspring, including variations in paternal nutrition, metabolic and hormonal status, or obesity itself[11]. In mice, however, males whose mothers consumed a HFD were heavier, diabetic and insulin resistant, and produced second-generation offspring who were insulin resistant, although not obese[12]. Whether this is a consequence of paternal *in utero* exposure or their adult sequelae of obesity and diabetes is unclear. In mice, a HFD also alters testicular gene expression[13]. Obesity affects sperm concentration, motility and morphology, and increases sperm DNA damage in humans[14]. Collectively, this indicates that fathers can initiate intergenerational transmission of obesity/metabolic diseases, induced indirectly or directly, such as through exposure to a HFD.

To test this hypothesis we mated male Sprague–Dawley founder rats fed either a HFD or a control diet (Table 1), with females consuming a control diet (Supplementary Table 1). As expected, HFD males had increased body weight, energy intake, adiposity and plasma leptin and liver mass (Fig. 1a–c and Table 1), but reduced skeletal muscle mass relative to body weight ($P = 0.017$). The HFD males were also glucose

Table 1 | Hormonal and metabolic parameters and pancreas morphology

Group and parameter	Control	HFD	*P* value
Fathers	$n = 8$	$n = 9$	
Body weight (g)	550 ± 13	705 ± 17	<0.0005
Length (cm)	26.8 ± 0.3	27.8 ± 0.3	0.017
Liver (g)	15.16 ± 0.43	19.51 ± 1.23	0.006
BAT (mg)	0.462 ± 0.026	0.779 ± 0.100	0.013
Mesenteric WAT (g)	4.76 ± 0.35	12.43 ± 1.23	<0.0005
Retroperitoneal WAT (g)	8.85 ± 0.60	30.85 ± 3.09	<0.0005
Gonadal WAT (g)	7.56 ± 0.32	20.83 ± 1.10	<0.0005
Sum of WAT (g)	21.17 ± 0.75	64.10 ± 4.84	<0.0005
Leptin (ng ml^{-1})	2.70 ± 0.30	13.26 ± 1.99	<0.0005
Glucose (mM)	4.71 ± 0.08	5.43 ± 0.16	0.002
Insulin (ng ml^{-1})	0.18 ± 0.02	0.47 ± 0.07	0.002
HOMA-IR	0.88 ± 0.11	2.29 ± 0.18	<0.0005
Female offspring	$n = 8$	$n = 9$	
Body weight (g)	253 ± 8	260 ± 5	0.92
Length (cm)	22.6 ± 0.2	22.3 ± 0.1	0.28
Liver (g)	7.15 ± 0.19	7.34 ± 0.16	0.46
BAT (mg)	0.19 ± 0.02	0.21 ± 0.01	0.43
Selected skeletal muscle mass (mg)	0.78 ± 0.02	0.77 ± 0.03	0.66
Mesenteric WAT (g)	2.14 ± 0.16	2.28 ± 0.20	0.59
Retroperitoneal WAT (g)	2.50 ± 0.37	2.81 ± 0.36	0.55
Gonadal WAT (g)	2.58 ± 0.10	2.80 ± 0.48	0.67
Sum of WAT (g)	6.76 ± 0.32	7.87 ± 0.89	0.28
Leptin (ng ml^{-1})	0.89 ± 0.09	1.06 ± 0.16	0.38
Triglyceride (mM)	0.92 ± 0.14	0.78 ± 0.12	0.46
NEFA (mEq l^{-1})	2.22 ± 0.12	2.59 ± 0.33	0.32
Pancreas morphology	$n = 7$	$n = 7$	
Total islet area (percentage pancreas area)	1.17 ± 0.09	0.90 ± 0.08	0.040
Per cent small islet (0–5,000 μm^2)	71.81 ± 0.82	76.08 ± 1.58	0.034
Per cent medium islet (5,001–10,000 μm^2)	10.04 ± 0.98	9.08 ± 0.79	0.46
Per cent large islet (>10,000 μm^2)	18.14 ± 0.48	14.84 ± 1.26	0.031
Total no. islet per mm^2 pancreas	1.56 ± 0.11	1.51 ± 0.13	0.80
No. small islet per mm^2 pancreas	1.12 ± 0.08	1.15 ± 0.11	0.80
No. medium islet per mm^2 pancreas	0.16 ± 0.02	0.14 ± 0.01	0.35
No. large islet per mm^2 pancreas	0.28 ± 0.02	0.23 ± 0.02	0.13
Total β-cell area (percentage pancreas area)	0.72 ± 0.06	0.58 ± 0.05	0.09

HFD, high fat diet. BW, body weight. BAT, brown adipose tissue. WAT, white adipose tissue. Sum of WAT, sum of mesenteric, retroperitoneal and gonadal WAT. Selected skeletal muscle mass, sum of anterior tibialis, extensor digital longus and soleus. HOMA-IR, homeostasis model assessment = fasting insulin (ng ml^{-1}) × fasting glucose (mM) / 22.5 × 0.0417. All results are expressed as mean ± s.e.m.

[1]Department of Pharmacology, School of Medical Sciences, University of New South Wales, New South Wales, Sydney 2052, Australia. [2]Ramaciotti Centre for Gene Function Analysis and School of Biotechnology and Biomolecular Sciences, University of New South Wales, New South Wales, Sydney 2052, Australia. [3]Garvan Institute of Medical Research, 384 Victoria St, Darlinghurst, Sydney 2010, Australia. [4]Department of Anatomy, School of Medical Sciences, University of New South Wales, New South Wales, Sydney 2052, Australia. [5]School of Paediatrics and Reproductive Health, University of Adelaide, South Australia 5005, Australia.

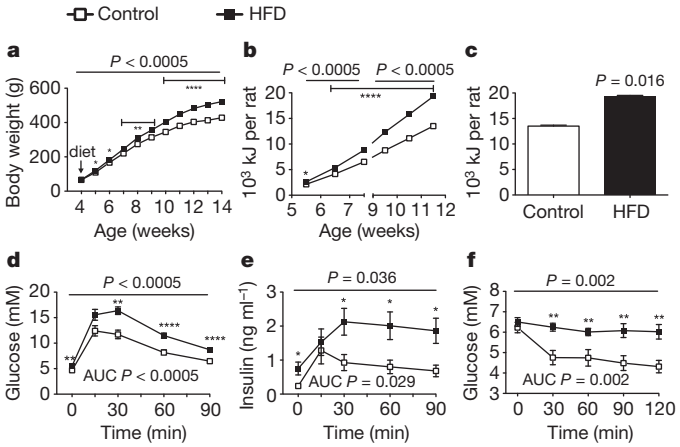

Figure 1 | HFD leads to adiposity, glucose intolerance and insulin resistance in fathers. **a**, Body-weight trajectories (control, HFD: $n = 8$ and 9, respectively). **b**, Cumulative energy intake ($n = 4$ and 5, respectively). **c**, Total energy intake ($n = 4$ and 5, respectively). **d**, Blood glucose during glucose tolerance test ($n = 8$ and 9, respectively). **e**, Plasma insulin during glucose tolerance test ($n = 7$ and 9, respectively). **f**, Blood glucose during insulin tolerance test (1 U kg^{-1}) ($n = 7$ and 9, respectively). Data are expressed as mean ± s.e.m. $*P < 0.05$, $**P < 0.01$, $****P < 0.0005$, versus control. P values for significant differences between male founder groups in repeated-measure analysis are shown at top of panel.

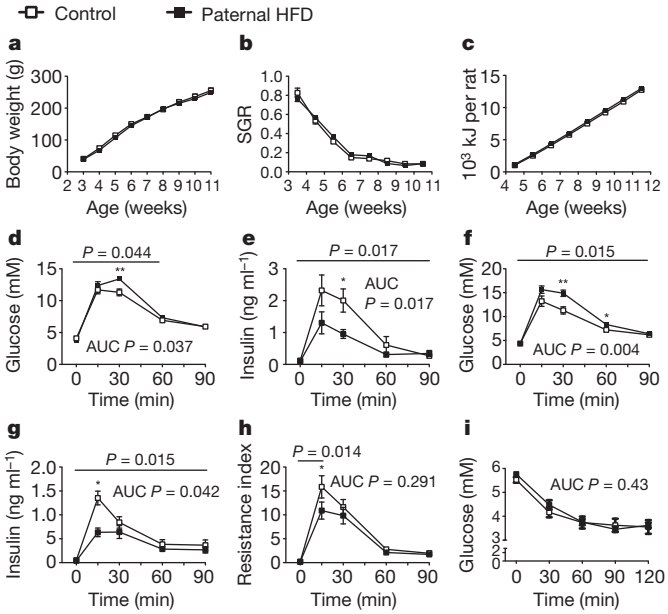

Figure 2 | Female offspring demonstrate impaired glucose tolerance and insulin secretion to a glucose challenge. **a**, Body weight (control, HFD: $n = 8$ and 9, respectively). **b**, Specific growth rate (SGR, change in body weight/body weight; $n = 8$ and 9, respectively). **c**, Cumulative energy intake ($n = 9$ and 7, respectively). **d**–**g** Blood glucose (**d**) and plasma insulin (**e**) during a glucose tolerance test at 6 weeks ($n = 8$ and 8, respectively) and 12 weeks (**f**, **g**) ($n = 5$ and 7, respectively). **h**, Insulin resistance index (glucose (mM) × insulin (ng ml^{-1}) × 0.0417/22.5) at 12 weeks. **i**, Blood glucose during an insulin tolerance test (0.5 U kg^{-1}) at 11 weeks ($n = 8$ and 9, respectively). Data are mean ± s.e.m. $*P < 0.05$, $**P < 0.01$, versus control. Significant differences between groups shown at top of panel.

intolerant and insulin resistant, showing raised blood glucose and plasma insulin at fasting and during a glucose tolerance test (Fig. 1d, e). The homeostasis model assessment of insulin resistance index (HOMA-IR; Table 1) was increased and the insulin-tolerance-test response blunted (Fig. 1f). Paternal HFD did not alter litter size or sex ratios.

In humans, paternal obesity is associated with low birth weight in offspring[6]. Here, day-1 body weight of female offspring of HFD fathers tended to be reduced (6.61 ± 0.15 versus 7.08 ± 0.26 g in controls; $n = 9$ and 8, respectively; $P = 0.07$); males (7.40 ± 0.21 versus 7.30 ± 0.20 g in controls; $n = 9$ and 8, respectively; $P = 0.74$). In girls, adiposity[15] and insulin resistance[16] closely resembled that of their obese fathers. As a pilot study identified significant impairment of glucose tolerance in female but not male offspring (S.F.N. and M.J.M., unpublished data), we further assessed females after weaning onto a control diet. A paternal HFD did not alter body weight, specific growth rate, energy intake (Fig. 2a–c) or energy efficiency (not shown) in female offspring.

In humans, paternal adiposity predicted that of their pre-menarcheal daughters[15]. Here, paternal HFD did not alter adiposity, muscle mass, fasting plasma leptin, triglyceride or non-esterified fatty acid (NEFA) concentrations in adult female offspring (Table 1). Either obesity may emerge later or it may not progress through the paternal lineage in rodents, as reported for those with undernourished[17] and HFD-fed[12] grandmothers.

Next we assessed glucose tolerance and its two key determinants, insulin secretion and sensitivity, in the female rat offspring. A paternal HFD did not alter fasting blood glucose (Fig. 2d, f) or plasma insulin (Fig. 2e, g) in female offspring, but increased the blood glucose rise (peak 13.6 ± 0.3 versus 12.3 ± 0.4 mM; $P = 0.043$) and reduced insulin secretion (peak 1.4 ± 0.3 versus 2.7 ± 0.4 ng ml^{-1}; $P = 0.016$) during a glucose tolerance test at 6 weeks (Fig. 2d, e). A similar pattern was observed at 12 weeks (Fig. 2f, g), but with a further impairment of glucose tolerance evidenced by a larger glucose peak (+10% to +23% versus control) and increased the area under the glucose curve during the glucose tolerance test, $AUC_{glucose}$ (+9% to +19%) in paternal HFD offspring. Insulin secretion during the first 30 min after glucose (insulinogenic index[18], $AUC_{insulin(0–30\,min)}/AUC_{glucose(0–30\,min)}$) was halved in offspring of HFD fathers (38.7 ± 5.8 versus 86.8 ± 7.3 ng mmol^{-1}; $P = 0.004$); but their insulin resistance index and response during the insulin tolerance test were unaltered (Fig. 2h, i).

We then examined islet and β-cell abundance, and performed genome-wide microarray analysis of isolated islets to explore the mechanisms of impaired insulin secretion. A paternal HFD reduced relative islet area (−23%; $P = 0.04$), mainly owing to reduced large islets (−18%; $P = 0.031$) and tended to reduce β-cell area ($P = 0.09$; Table 1) in offspring, implying impaired β-cell replication. We also observed an increase in small islets (+6%; $P = 0.034$; Table 1) in the offspring of HFD fathers, indicating a compensatory response to maintain normal β-cell mass. We propose that limited β-cell reserve in the female offspring of HFD fathers is sufficient to maintain normal fasting glucose and insulin levels, but inadequate to preserve glucose-stimulated insulin secretion and glucose tolerance.

A paternal HFD altered the expression of 77 genes (21 upregulated, 56 downregulated, $P < 0.001$; Supplementary Table 2) in adult female offspring; 642 genes at $P < 0.01$ had enriched gene ontology terms belonging to regulatory pathways associated with insulin and glucose metabolism, that is, cation and ATP binding, cytostructure and intracellular transport (Supplementary Fig. 1). Broader Kyoto Encyclopedia of Genes and Genomes (KEGG) pathway analysis of 2,492 genes ($P < 0.05$) revealed the involvement of calcium-, MAPK- and Wnt-signalling, apoptosis and the cell cycle (Table 2). Molecular networks were also identified, including direct interactions between members of Jak–Stat and MAPK signalling (Supplementary Figs 2 and 3 and Supplementary Table 3) and other functionally enriched pathways (Supplementary Table 3). Overall, these molecular findings are consistent with the alterations in pancreas morphology and indicate impaired insulin-granule exocytosis[19,20]. The greatest fold difference in gene expression was observed in *Il13ra2*, part of the Jak–Stat signalling pathway (Table 2). *Il13ra2* is expressed in and modulates growth and invasion of various pancreatic cancer cell lines[21] and is upregulated by TNF-α (*Tnf*)[22]. Quantitative polymerase chain reaction with

Table 2 | Differentially expressed islet genes ($P < 0.05$) of female offspring in functionally enriched pathways

Gene symbol	RefSeq	Probe-set ID	Mean		HFD versus control	
			HFD* ($n = 5$)	Control* ($n = 6$)	Fold change†	*P* value
Ca signalling (KEGG 04020)						
Adrb1 (d)	NM_012701	10716262	5.51	5.70	−1.14	0.035
Chrm1 (d)	NM_080773	10713581	6.01	6.17	−1.12	0.041
Htr6 (d)	NM_024365	10882383	5.50	5.69	−1.14	0.014
Htr7 (d)	NM_022938	10729825	5.12	5.37	−1.19	0.004
Adcy2 (d)	NM_031007	10793338	5.58	5.71	−1.09	0.024
Cacna1e (d)	NM_019294	10768765	4.85	5.01	−1.11	0.026
Ryr1 (d)	ENSRNOT00000027893	10720308	5.65	5.78	−1.10	0.020
Camk2a (d)	NM_012920	10802026	5.47	5.58	−1.07	0.036
Pde1b (d)	NM_022710	10899676	5.88	6.13	−1.19	0.039
Sphk1 (d)	NM_133386	10739796	5.38	5.59	−1.15	0.022
Grin1 (u)	NM_017010	10843400	7.16	6.92	1.18	0.006
Vdac3 (u)	NM_031355	10789127	10.66	10.52	1.11	0.010
Phkg2 (u)	NM_080584	10711127	8.15	8.06	1.07	0.019
Pde1c (u)	NM_031078	10862700	7.00	6.68	1.26	0.007
MAPK signalling (KEGG 04010)						
Cacna1e (d)	NM_019294	10768765	4.85	5.01	−1.11	0.026
Cacna2d3 (d)	NM_175595	10789819	5.14	5.26	−1.09	0.032
Cacna2d4 (d)	ENSRNOT00000010746	10858218	5.19	5.32	−1.09	0.014
Tnf (d)	NM_012675	10828021	5.21	5.50	−1.22	0.019
Fos (d)	NM_022197	10886031	7.91	8.82	−1.87	0.014
Ptpn7 (d)	NM_145683	10764196	5.28	5.44	−1.12	0.004
Map3k4 (d)	NM_001107456	10717995	6.24	6.53	−1.22	0.005
Rap1a (u)	NM_001005765	10825727	8.81	8.69	1.09	0.046
Rasa1 (u)	NM_013135	10820245	9.33	9.25	1.06	0.016
Map2k4 (u)	NM_001030023	10743668	8.35	8.22	1.09	0.002
Crk (u)	NM_019302	10736033	9.25	9.19	1.04	0.047
Casp3 (u)	NM_012922	10791652	8.60	8.53	1.05	0.050
Daxx (u)	NM_080891	10831792	7.14	7.00	1.10	0.031
Il1rl1 (u)	NM_001127689	10922857	5.60	4.79	1.75	0.025
Mknk2 (u)	NM_001011985	10893744	7.72	7.55	1.13	0.050
Wnt signalling (KEGG 04310)						
Wnt9a (d)	NM_001105783	10733966	5.83	6.03	−1.15	0.003
Wnt9b (d)	NM_001107055	10748113	6.19	6.39	−1.15	0.001
Fzd9 (d)	NM_153305	10757698	6.02	6.15	−1.09	0.014
Ctnnb1 (u)	NM_053357	10914371	10.07	9.96	1.08	0.049
Ppp2r5a (u)	NM_001107891	10770721	9.52	9.36	1.12	0.036
Skp1 (u)	NM_001007608	10733430	10.81	10.64	1.12	0.024
Cul1 (u)	NM_001108627	10855163	10.03	9.96	1.05	0.041
Rock1 (u)	NM_031098	10803158	9.29	9.20	1.06	0.016
Apoptosis (KEGG 04210)						
Tnf (d)	NM_012675	10828021	5.21	5.50	−1.22	0.019
Bcl2l1 (d)	NM_031535	10850826	7.01	7.07	−1.04	0.045
Il1rl1 (u)	NM_001127689	10922857	5.60	4.79	1.75	0.025
Prkar2a (u)	NM_019264	10913228	8.64	8.51	1.09	0.046
Casp3 (u)	NM_012922	10791652	8.60	8.53	1.05	0.050
Xiap (u)	AF304334	10921195	9.98	9.85	1.10	0.020
Aifm1 (u)	NM_031356	10939595	7.98	7.83	1.11	0.029
Cell cycle (KEGG 04110)						
Orc1l (d)	NM_177931	10870791	4.47	4.72	−1.19	0.015
Smc1b (d)	NM_001130498	10905944	3.77	4.00	−1.18	0.032
Skp1 (u)	NM_001007608	10733430	10.81	10.64	1.12	0.024
Cul1 (u)	NM_001108627	10855163	10.03	9.96	1.05	0.041
Prkdc (u)	NM_001108327	10755897	8.37	8.29	1.05	0.025
Stag1 (u)	NM_001108179	10912525	8.06	7.89	1.12	0.003
E2f3 (u)	NM_001137626	10798213	5.85	5.59	1.20	0.017
Jak–Stat signalling (KEGG 04630)						
Mpl (d)	ENSRNOT00000042602	10879267	4.65	4.99	−1.27	0.001
Stat1 (d)	ENSRNOT00000052121	10927873	7.18	7.43	−1.19	0.006
Ifnb1 (d)	NM_019127	10877952	4.10	4.31	−1.16	0.012
Jak3 (d)	NM_012855	10787364	6.56	6.77	−1.15	0.035
Il9 (d)	NM_001105747	10793945	5.73	5.92	−1.14	0.022
Ifna1 (d)	NM_001014786	10877972	5.56	5.73	−1.13	0.013
Ifna1 (d)	NM_001014786	10877968	5.37	5.52	−1.11	0.032
Socs3 (d)	NM_053565	10749372	6.08	6.24	−1.11	0.033
Il23a (d)	NM_130410	10899749	6.11	6.22	−1.08	0.012
Bcl2l1 (d)	NM_031535	10850826	7.01	7.07	−1.04	0.045
Il13ra2 (u)	NM_133538	10937279	3.77	2.95	1.76	0.018
Il13ra2 (u)	NM_133538	10937292	3.97	3.16	1.75	0.033

U, upregulated gene; d, downregulated gene.
* Values represent fluorescent intensity of probe-set and are presented in log 2 space.
† Fold change is gene expression in offspring of HFD father relative to control.

reverse transcription (RT–PCR) confirmed upregulation of messenger RNA expression ($n = 5$ per group) of *Il13ra2* (+6.3; $P < 0.05$) and *Ikbke* (+2.9; $P < 0.01$) and a decrease in *Fos* (−4.0; $P < 0.05$) in the islets of offspring of HFD fathers. To determine if epigenetic mechanisms could contribute to the altered *Il13ra2* expression, we performed bisulphite sequencing of a region proximal to the transcription start site.

Methylation at cytosine −960 of *Il13ra2* was reduced in HFD offspring (8.9 ± 2.2%) compared to controls (33.6 ± 4.0%, $P < 0.001$). Cytosine −960 was found to be located in a putative binding site for the T-cell factor-1A and NF-X, the latter being a methylated DNA-binding protein[23]. This epigenetic modification of *Il13ra2*, a gene that is part of key molecular networks (Table 2, Supplementary Table 3 and Supplementary Fig. 4), indicates that a paternal HFD alters offspring islet function, in part by affecting the epigenome of offspring.

In humans, paternal insulin resistance/diabetes is inversely associated with offspring birthweight[24,25] and increases subsequent risk of diabetes[24]. Although genetic factors may contribute[26], our findings show that paternal exposure to a HFD can induce a similar phenotype in offspring, identifying an additional and influential pathway. Notably, the impaired glucose tolerance and insulin secretion, in the absence of obesity, in these female offspring indicate that a paternal HFD acts to particularly target the endocrine pancreas and β-cells early in offspring. Whether similar defects emerge in male offspring remains to be determined.

Paternal lifestyle and particular environmental factors can affect spermatogenesis at the level of germ and Sertoli cells[27] and the composition of seminal fluid[28]. Increased testicular temperature resulting from fat accumulation and increased dietary fat and by-products of cell metabolism can be directly genotoxic to germ cells within the mature testis, leading to increased DNA damage through oxidative injury[29]. Furthermore, hyperleptinaemia, hyperinsulinaemia and the relative hypogonadotrophic hypogonadism in obese males may consequently affect spermatogenesis[30]. A HFD may also interfere with Sertoli-cell proliferation, and the integrity of the blood–testis barrier, thus affecting DNA reprogramming of the gamete[29]. A critical unanswered question, given the rising obesity epidemic in children, is whether early onset and prolonged HFD exposure may also affect gametogenesis and thereby offspring.

To our knowledge, this is the first direct demonstration in any species that a paternal environmental exposure, HFD consumption, can induce intergenerational transmission of impaired glucose–insulin homeostasis in their female offspring. The underlying mechanisms seem to include epigenetic modifications, the functional implications of which remain to be elucidated. These findings extend the concept of developmental and adaptive plasticity to include a paternal role in the early life origins of disease and amplification of the diabetes epidemic.

METHODS SUMMARY

Animal experiments. Litters from eight control and nine HFD fathers were included; one animal per litter was used for each test. Experimental protocols were approved by the Animal Care and Ethics Committee, University of New South Wales.
Microarray gene expression analysis. Total islet mRNA was extracted using miRNeasy Mini kits (Qiagen). Samples from six control and five HFD offspring, each from different fathers, with RNA integrity number (RIN, Agilent) ≥7.5 were selected for transcriptomics using Affymetrix GeneChip Rat Gene ST 1.0 arrays.
Statistical analyses. Phenotype data were analysed using SPSS 16.0 after log transformation or square-root transformation unless raw data were normally distributed. Single time measurements were analysed by two-tailed Student's *t*-test or Mann–Whitney *U* test, and time-courses were analysed by repeated-measures ANOVA.

Full Methods and any associated references are available in the online version of the paper at www.nature.com/nature.

Received 27 December 2009; accepted 10 September 2010.

1. Wang, Y. & Lobstein, T. Worldwide trends in childhood overweight and obesity. *Int. J. Pediatr. Obes.* **1,** 11–25 (2006).
2. Pinhas-Hamiel, O. & Zeitler, P. The global spread of type 2 diabetes mellitus in children and adolescents. *J. Pediatr.* **146,** 693–700 (2005).
3. Whitaker, R. C., Wright, J. A., Pepe, M. S., Seidel, K. D. & Dietz, W. H. Predicting obesity in young adulthood from childhood and parental obesity. *N. Engl. J. Med.* **337,** 869–873 (1997).
4. Morris, M. Early life influences on obesity risk: maternal overnutrition and programming of obesity. *Expert Rev. Endocrinol. Metab.* **4,** 625–637 (2009).
5. Tarquini, B., Tarquini, R., Perfetto, F., Cornelissen, G. & Halberg, F. Genetic and environmental influences on human cord blood leptin concentration. *Pediatrics* **103,** 998–1006 (1999).
6. Power, C., Li, L., Manor, O. & Davey Smith, G. Combination of low birth weight and high adult body mass index: at what age is it established and what are its determinants? *J. Epidemiol. Community Health* **57,** 969–973 (2003).
7. Bouchard, C. Childhood obesity: are genetic differences involved? *Am. J. Clin. Nutr.* **89,** 1494S–1501S (2009).
8. Guo, Y. F. *et al.* Assessment of genetic linkage and parent-of-origin effects on obesity. *J. Clin. Endocrinol. Metab.* **91,** 4001–4005 (2006).
9. Le Stunff, C., Fallin, D. & Bougneres, P. Paternal transmission of the very common class I *INS* VNTR alleles predisposes to childhood obesity. *Nature Genet.* **29,** 96–99 (2001).
10. Gluckman, P. D. *et al.* Towards a new developmental synthesis: adaptive developmental plasticity and human disease. *Lancet* **373,** 1654–1657 (2009).
11. Li, L., Law, C., Lo Conte, R. & Power, C. Intergenerational influences on childhood body mass index: the effect of parental body mass index trajectories. *Am. J. Clin. Nutr.* **89,** 551–557 (2009).
12. Dunn, G. A. & Bale, T. L. Maternal high-fat diet promotes body length increases and insulin insensitivity in second-generation mice. *Endocrinology* **150,** 4999–5009 (2009).
13. Ghanayem, B. I., Bai, R., Kissling, G. E., Travlos, G. & Hoffler, U. Diet-induced obesity in male mice is associated with reduced fertility and potentiation of acrylamide-induced reproductive toxicity. *Biol. Reprod.* **82,** 96–104 (2009).
14. Kasturi, S. S., Tannir, J. & Brannigan, R. E. The metabolic syndrome and male infertility. *J. Androl.* **29,** 251–259 (2008).
15. Figueroa-Colon, R., Arani, R. B., Goran, M. I. & Weinsier, R. L. Paternal body fat is a longitudinal predictor of changes in body fat in premenarcheal girls. *Am. J. Clin. Nutr.* **71,** 829–834 (2000).
16. Leibel, N. I., Baumann, E. E., Kocherginsky, M. & Rosenfield, R. L. Relationship of adolescent polycystic ovary syndrome to parental metabolic syndrome. *J. Clin. Endocrinol. Metab.* **91,** 1275–1283 (2006).
17. Jimenez-Chillaron, J. C. *et al.* Intergenerational transmission of glucose intolerance and obesity by *in utero* undernutrition in mice. *Diabetes* **58,** 460–468 (2009).
18. Sone, H. & Kagawa, Y. Pancreatic β cell senescence contributes to the pathogenesis of type 2 diabetes in high-fat diet-induced diabetic mice. *Diabetologia* **48,** 58–67 (2005).
19. Henquin, J. C., Nenquin, M., Ravier, M. A. & Szollosi, A. Shortcomings of current models of glucose-induced insulin secretion. *Diabetes Obes. Metab.* **11** (suppl. 4), 168–179 (2009).
20. Wang, Z. & Thurmond, D. C. Mechanisms of biphasic insulin-granule exocytosis—roles of the cytoskeleton, small GTPases and SNARE proteins. *J. Cell Sci.* **122,** 893–903 (2009).
21. Fujisawa, T., Joshi, B., Nakajima, A. & Puri, R. K. A novel role of interleukin-13 receptor α2 in pancreatic cancer invasion and metastasis. *Cancer Res.* **69,** 8678–8685 (2009).
22. David, M., Bertoglio, J. & Pierre, J. TNF-α potentiates IL-4/IL-13-induced IL-13Rα2 expression. *Ann. NY Acad. Sci.* **973,** 207–209 (2002).
23. Zhang, X. Y. *et al.* The major histocompatibility complex class II promoter-binding protein RFX (NF-X) is a methylated DNA-binding protein. *Mol. Cell. Biol.* **13,** 6810–6818 (1993).
24. Lindsay, R. S. *et al.* Type 2 diabetes and low birth weight: the role of paternal inheritance in the association of low birth weight and diabetes. *Diabetes* **49,** 445–449 (2000).
25. Hypponen, E., Smith, G. D. & Power, C. Parental diabetes and birth weight of offspring: intergenerational cohort study. *Br. Med. J.* **326,** 19–20 (2003).
26. Hattersley, A. T. & Tooke, J. E. The fetal insulin hypothesis: an alternative explanation of the association of low birthweight with diabetes and vascular disease. *Lancet* **353,** 1789–1792 (1999).
27. Sharpe, R. M. Environmental/lifestyle effects on spermatogenesis. *Phil. Trans. R. Soc. Lond. B* **365,** 1697–1712 (2010).
28. Robertson, S. A. Seminal plasma and male factor signalling in the female reproductive tract. *Cell Tissue Res.* **322,** 43–52 (2005).
29. Aitken, R. J., Koopman, P. & Lewis, S. E. Seeds of concern. *Nature* **432,** 48–52 (2004).
30. Du Plessis, S. S., Cabler, S., McAlister, D. A., Sabanegh, E. & Agarwal, A. The effect of obesity on sperm disorders and male infertility. *Nature Rev. Urol.* **7,** 153–161 (2010).

Supplementary Information is linked to the online version of the paper at www.nature.com/nature.

Acknowledgements This work is supported by the National Health and Medical Research Council (NHMRC) of Australia (M.J.M.). S.F.N. is supported by Ministry of Higher Education and National University of Malaysia, R.C.Y.L. is supported by the NHMRC Peter Doherty Fellowship.

Author Contributions S.F.N. and M.J.M. designed the study. S.F.N. performed animal work, histology, islet harvest and RNA extraction, data analysis and wrote the manuscript. M.J.M. supervised the project and wrote the manuscript. R.C.Y.L. conducted microarray data analysis. D.R.L. assisted with islet harvest. R.B. conducted bisulphite sequencing and DNA methylation analysis. J.A.O. conducted ingenuity analysis and wrote the manuscript. All authors contributed to data interpretation, reviewed the manuscript and approved the final version.

Author Information Gene expression data have been deposited in the National Center for Biotechnology Information Gene Expression Omnibus (GEO; http://www.ncbi.nim.nih.gov/geo) and are accessible using GEO series accession number GSE19877. Reprints and permissions information is available at www.nature.com/reprints. The authors declare no competing financial interests. Readers are welcome to comment on the online version of this article at www.nature.com/nature. Correspondence and requests for materials should be addressed to M.J.M. (m.morris@unsw.edu.au).

METHODS

Animal care. Sprague–Dawley rats from the Animal Resource Centre were housed at 22 ± 2 °C, on a 12:12 h light:dark cycle. Male F_0 founders were assigned to a HFD (SF01-025, SF03-020; 40.7%, 43% energy as fat; Speciality Feeds) or control (Gordon's Stockfeeds) diet at 4 weeks of age. At 13 weeks, HFD males were 22% heavier (522 ± 11 versus 428 ± 13 g, $P = 0.008$); mating with females consuming control diet commenced at 14 weeks. During mating, one male and one female were housed together, with free access to control diet from 0800–1800 h, for 8 consecutive days. Males returned to their cages overnight to continue their assigned diets, whereas females consumed control diet throughout mating, gestation and lactation. Male and female founders were killed in the fasting state shortly after litters were harvested. Females mated with the two paternal groups did not differ in body weight, adiposity, fasting blood glucose, insulin and HOMA-IR (Supplementary Table 1). Only litter sizes between 9–16 were included and litters were standardized to 12 pups at day 1 within father groups, to control for intrauterine and postnatal nutrition. Phenotypic data (body weight, specific growth rate, glucose tolerance, insulin tolerance, post mortem) from one offspring per father, chosen at random, were generated. At week 13, animals were killed and islets were generated from 5 HFD and 6 control offspring, each from a different father. Littermates were killed for pancreas histology and post-mortem analysis at week 14.

Body weight and energy intake were monitored weekly, the latter by collecting and weighing food remaining after 24 h. Energy intake was averaged across animals housed with 3–4 per cage to reduce stress. Specific growth rate (SGR; weight gain between two time points divided by previous body weight[31]) and energy efficiency (weight gain divided by energy intake between the two time points) were calculated.

Blood glucose (Accu check Advantage glucometer; Roche), plasma leptin and insulin (Linco radioimmunoassay), plasma NEFA (Wako) and triglyceride (Roche colorimetric enzymatic assay) were determined.

Glucose and insulin tolerance tests. Glucose tolerance test was performed after a 15-h overnight fast and insulin tolerance test was performed 2 h after food removal. Glucose (2 g kg^{-1} body weight) and insulin (Actrapid, Novo Nordisk; 1 U kg^{-1} for fathers and 0.5 U kg^{-1} for offspring based on their predicted insulin resistance) were administered intraperitoneally. Separate cohorts of littermates underwent a glucose tolerance test for blood glucose and plasma insulin measures at 6 weeks of age, to reduce stress associated with blood sampling.

Immunohistochemistry and morphometric analysis. Three fixed pancreas sections (5 μm) per animal per test, 200 μm apart, were stained with polyclonal guinea-pig anti-swine insulin primary antibody followed by goat anti-rabbit immunoglobulin secondary antibody (DAKO). Adjacent sections were stained with haematoxylin and eosin. All slides were scanned using Aperio ScanScope XT Slide Scanner. Pancreas, islet and β-cell areas were determined using ImageJ 1.40 software (http://rsb.info.nih.gov/ij/). Islets were classified into small (1–5,000 μm^2), medium (5,001–10,000 μm^2) and large (>10,000 μm^2), respectively[32].

Islet isolation. Islets were harvested by standard techniques with cannulation of the pancreatic duct of anaesthetized rats[33–35] after an overnight fast.

Islets transcriptomics. Affymetrix probe-set data were normalized using the robust multi-array average (RMA) method[36], which can yield attenuated estimates of differential expression for genes at low expression levels, albeit with high precision. Gene expression levels were compared using one-way ANOVA. This yielded 77, 642 and 2,492 differentially expressed genes at unadjusted $P < 0.001$, $P < 0.01$ and $P < 0.05$ levels, respectively. Differentially expressed genes ($P < 0.01$) were functionally annotated according to gene ontology terms and enriched terms were calculated using DAVID[37,38] (Supplementary Fig. 1). In addition, we hierarchically clustered[39] differentially expressed genes based on Euclidean distance to look for possible co-regulated pathways affecting islet metabolism. We also mapped differentially expressed genes at $P < 0.05$ to KEGG[40].

Quantitative RT–PCR. Total islet RNA (one offspring per father; $n = 5$, HFD; $n = 5$, control), extracted using miRNeasy Mini kit (Qiagen), was used as a template for complementary DNA synthesis, using SuperScript III first strand synthesis (Invitrogen) with random hexamers. mRNA expression was determined using quantitative RT–PCR (Stratagene Mx3000P, Agilent) using primer sequences summarized in Supplementary Table 4 and Platinum SYBR Green SuperMix UDG (Invitrogen), normalized against β actin.

Molecular network generation using Ingenuity pathways analysis. Networks were generated through Ingenuity pathways analysis (Ingenuity Systems, http://www.ingenuity.com). Briefly, differentially expressed genes at $P < 0.01$ or $P < 0.05$ and corresponding fold changes were used; the number of networks and eligible molecules per network is limited to 25 and 35, respectively. Networks were algorithmically generated based on their connectivity and ranked by score (negative exponent of the right-tailed Fisher's exact test result). Molecules are represented as nodes, and the biological relationship between two nodes as an edge (line). Nodes are displayed using various shapes that represent the functional class of the gene product, whereas edges describe the nature of the relationship between the nodes, as defined in Ingenuity Systems.

DNA methylation analysis by bisulphite sequencing. Bisulphite treatment was performed as described[41]. One microgram of NaOH-denaturated DNA was embedded in 2% low-melting-point agarose solution; bisulphite solution (Sigma) was added, followed by 4 h of incubation at 50 °C under light exclusion. Treatment was terminated by equilibration against Tris-EDTA and 0.2 M NaOH, DNA was washed with distilled H_2O. *Il13ra2*, forward primer TAAATTAAAA TTTTAAAAATTGAAAAGTAT, reverse primer AAATAAAAAAAACTCATA AAATCAAC. The obtained PCR fragments were purified using MinElute Gel Extraction Kit (Qiagen) and cloned into PCR-TOPO vector using TOPO TA Cloning kit (Invitrogen). Individual clones were grown and plasmids purified using PureLink Miniprep kit (Invitrogen). For each animal eight to nine clones were sequenced using T7 promoter primer on an ABI 3730xl DNA Analyser platform at the Ramaciotti Center. Results were analysed using Methtools 2.0[42].

Statistical analysis. Results are expressed as mean ± s.e.m. $P < 0.05$ was considered statistically significant.

31. Prior, L. J., Velkoska, E., Watts, R., Cameron-Smith, D. & Morris, M. J. Undernutrition during suckling in rats elevates plasma adiponectin and its receptor in skeletal muscle regardless of diet composition: a protective effect? *Int. J. Obes. (Lond)* **32,** 1585–1594 (2008).
32. Chamson-Reig, A., Thyssen, S. M., Arany, E. & Hill, D. J. Altered pancreatic morphology in the offspring of pregnant rats given reduced dietary protein is time and gender specific. *J. Endocrinol.* **191,** 83–92 (2006).
33. Lacy, P. E. & Kostianovsky, M. Method for the isolation of intact islets of Langerhans from the rat pancreas. *Diabetes* **16,** 35–39 (1967).
34. Laybutt, D. R. *et al.* Increased expression of antioxidant and antiapoptotic genes in islets that may contribute to β-cell survival during chronic hyperglycemia. *Diabetes* **51,** 413–423 (2002).
35. Laybutt, D. R. *et al.* Critical reduction in β-cell mass results in two distinct outcomes over time. Adaptation with impaired glucose tolerance or decompensated diabetes. *J. Biol. Chem.* **278,** 2997–3005 (2003).
36. Irizarry, R. A. *et al.* Exploration, normalization, and summaries of high density oligonucleotide array probe level data. *Biostatistics* **4,** 249–264 (2003).
37. Huang, da W., Sherman, B. T. & Lempicki, R. A. Systematic and integrative analysis of large gene lists using DAVID bioinformatics resources. *Nature Protocols* **4,** 44–57 (2009).
38. Dennis, G. Jr *et al.* DAVID: database for annotation, visualization, and integrated discovery. *Genome Biol.* **4,** P3 (2003).
39. Saeed, A. I. *et al.* TM4: a free, open-source system for microarray data management and analysis. *Biotechniques* **34,** 374–378 (2003).
40. Kanehisa, M. & Goto, S. KEGG: Kyoto encyclopedia of genes and genomes. *Nucleic Acids Res.* **28,** 27–30 (2000).
41. Olek, A., Oswald, J. & Walter, J. A modified and improved method for bisulphite based cytosine methylation analysis. *Nucleic Acids Res.* **24,** 5064–5066 (1996).
42. Grunau, C., Schattevoy, R., Mache, N. & Rosenthal, A. MethTools—a toolbox to visualize and analyze DNA methylation data. *Nucleic Acids Res.* **28,** 1053–1058 (2000).